

# Magnetic Fields in Protoplanetary Disks

Mark Wardle

© Springer-Verlag ●●●●

**Abstract** Magnetic fields likely play a key role in the dynamics and evolution of protoplanetary disks. They have the potential to efficiently transport angular momentum by MHD turbulence or via the magnetocentrifugal acceleration of outflows from the disk surface. Magnetically-driven mixing has implications for disk chemistry and evolution of the grain population, and the effective viscous response of the disk determines whether planets migrate inwards or outwards. However, the weak ionisation of protoplanetary disks means that magnetic fields may not be able to effectively couple to the matter. I examine the magnetic diffusivity in a minimum solar nebula model and present calculations of the ionisation equilibrium and magnetic diffusivity as a function of height from the disk midplane at radii of 1 and 5 AU. Dust grains tend to suppress magnetic coupling by soaking up electrons and ions from the gas phase and reducing the conductivity of the gas by many orders of magnitude. However, once grains have grown to a few microns in size their effect starts to wane and magnetic fields can begin to couple to the gas even at the disk midplane. Because ions are generally decoupled from the magnetic field by neutral collisions while electrons are not, the Hall effect tends to dominate the diffusion of the magnetic field when it is able to partially couple to the gas, except at the disk surfaces where the low density of neutrals permits the ions to remain attached to the field lines.

For a standard population of  $0.1\mu\text{m}$  grains the active surface layers have a combined column  $\Sigma_{\text{active}} \approx 2\text{ g cm}^{-2}$  at 1 AU; by the time grains have aggregated to  $3\mu\text{m}$ ,  $\Sigma_{\text{active}} \approx 80\text{ g cm}^{-2}$ . Ionisation in the active layers is dominated by stellar x-rays. In the absence of grains, x-rays maintain magnetic coupling to 10% of

the disk material at 1 AU (i.e.  $\Sigma_{\text{active}} \approx 150\text{ g cm}^{-2}$ ). At 5 AU  $\Sigma_{\text{active}} \approx \Sigma_{\text{total}}$  once grains have aggregated to  $1\mu\text{m}$  in size.

**Keywords** accretion, accretion disks – MHD – molecular processes – stars: formation

## 1 Introduction

Magnetic fields may efficiently transport angular momentum in protoplanetary disks either via MHD turbulence driven by the magnetorotational instability (Balbus & Hawley 1991; Hawley, Gammie & Balbus 1994), by accelerating a wind from the disk surfaces (Blandford & Payne 1982; Wardle & Königl 1993), or by looping above the disk surface and linking different radii. Advection and/or stirring by magnetically-driven turbulence affects disk chemistry (e.g. Semenov, Wiebe & Henning 2006; Ilgner & Nelson 2006), the aggregation and settling of small particles that are the preliminary stages of planet building (Johansen & Klahr 2005; Turner et al. 2006; Fromang & Papaloizou 2006; Ciesla 2007), and magnetic activity at the disk surface may produce a corona (e.g. Fleming & Stone 2003) and affect observational signatures of protoplanetary disks. A magnetically-mediated effective viscosity would also determine the response of the disk to the gravitational disturbances of forming planets, modifying the balance between the torques applied by the outer and inner neighbouring regions of the disk and therefore the rate and direction of planetary migration (Matsumura & Pudritz 2003; Johnson, Goodman & Menou 2006; Chambers 2006). Finally, magnetic fields are likely to play a role in giant planet formation and the formation and evolution of their satellite systems (Quillen & Trilling 1998; Fendt 2003).

---

Mark Wardle

Department of Physics, Macquarie University, Sydney NSW 2109, Australia

One critical uncertainty is the magnitude and nature of the coupling between magnetic fields and protoplanetary disks, which are very weakly ionised on account of the self-shielding against ionising sources provided by their high column density, and by rapid recombinations because of their high number densities. In addition the mobility of charged particles is reduced by the relatively high density, and dust grains sweep up charges and render them effectively immobile. Indeed, magnetic fields were expected to be negligible in protoplanetary disks, as extremely high diffusion was thought to eliminate the magnetic gradients responsible for magnetic stresses except at the disk surfaces (e.g. Hayashi 1981). But these expectations are too pessimistic. At any given radius in the disk the density declines rapidly with height because of tidal squeezing by the gravitational field of the central star. The corresponding rapid decline in diffusivity towards the disk surface is aided by external ionisation by cosmic rays and by stellar x-rays which dominate cosmic rays by five orders of magnitude within a few  $\text{g cm}^{-2}$  of the disk surface (Glassgold, Najita & Igea 1997; Igea & Glassgold 1999), so that at least the surface layers may be magnetically active (Gammie 1996; Wardle 1997). In addition, the Hall effect provides a dissipationless diffusion pathway that can maintain field gradients under a much broader range of conditions than would otherwise occur (Wardle & Ng 1999; Wardle 1999; Balbus & Terquem 2001). Finally, aggregation and settling of grains increases the number and mobility of charged species in the gas phase and reduces diffusivity to the point that magnetic stresses are important even at the disk midplane (Sano & Stone 2002).

Here I explore the nature and magnitude of magnetic diffusion in protoplanetary disks through calculations of the ionisation equilibrium in a stratified disk exposed to cosmic rays and to x-rays from the central star.

## 2 Minimum-mass solar nebula

To estimate the degree of coupling of magnetic fields to the matter in protoplanetary disks we first need a notional model for the physical conditions within the disk. I adopt the minimum-mass solar nebula model (Weidenschilling 1977; Hayashi 1981), in which the surface density of the solar nebula,  $\Sigma$ , is estimated by adding sufficient hydrogen and helium to the solid bodies in the solar system to recover standard interstellar abundances and spreading this material smoothly in a disk. This yields an estimate of the minimum surface density needed in the solar nebula to form the solar system,

$$\Sigma \approx 1700 r_{\text{AU}}^{-3/2} \text{ g cm}^{-2}, \quad (1)$$

where  $r_{\text{AU}}$  is the radial distance  $r$  from the Sun in astronomical units. The disk mass enclosed within  $r$  is

$$M_D = \int_{r_{\text{min}}}^r 2\pi r' \Sigma dr' \approx 0.024 \left( \frac{r}{100 \text{ AU}} \right)^{1/2} M_{\odot}, \quad (2)$$

where  $r$  is assumed to be much greater than the inner disk radius  $r_{\text{min}}$ . The temperature profile of the disk is estimated by considering the thermal balance for a black body of radius  $a$  at a distance  $r$  from the Sun,

$$\frac{L_{\odot}}{4\pi r^2} \pi a^2 = 4\pi a^2 \sigma_{\text{SB}} T^4, \quad (3)$$

where  $\sigma_{\text{SB}}$  is the Stefan-Boltzmann constant, which yields

$$T \approx 280 r_{\text{AU}}^{-1/2} \text{ K}. \quad (4)$$

These rough estimates of the distribution of matter and temperature are broadly consistent with continuum observations of protoplanetary disks around low mass stars, albeit with resolutions equivalent to  $\sim 100$  AU scales (e.g. Kitamura et al. 2002; Andrews & Williams 2005).

The isothermal sound speed in the disk implied by this temperature profile is

$$c_s \approx 0.99 r_{\text{AU}}^{-1/4} \text{ km s}^{-1} \quad (5)$$

which is small compared to the local Keplerian speed  $v_K$ , so the disk is thin (see eq [8] below). Here I have adopted a mean molecular weight of  $7/3 m_p$  appropriate for a mixture of 80%  $\text{H}_2$  and 20% He by number. Toomre's  $Q$  parameter (Toomre 1964) is

$$Q = \frac{c_s \Omega}{\pi G \Sigma} \approx 56 r_{\text{AU}}^{-1/4}, \quad (6)$$

where  $\Omega = v_K/r$  is the local Keplerian frequency and  $G$  is the gravitational constant, so the disk is not unstable to self gravity (as expected given  $M_D \ll M_{\odot}$ ). Of course this represents the *minimum* solar nebula; the surface density could be increased by factor of  $\sim 30$  between 1–100 AU before the disk becomes gravitationally unstable (e.g. Durisen et al. 2007), although as noted above large disk masses do not seem to be present in low mass YSOs.

Assuming that the temperature does not depend on height  $z$  above the disk midplane, the balance between tidal squeezing by the central object and its internal pressure imply that the gas density is stratified as

$$\rho(r, z) = \rho_0(r) \exp\left(-\frac{z^2}{2h^2}\right), \quad (7)$$

where the disk scale height  $h$  is given by

$$\frac{h}{r} = \frac{c_s}{v_K} \approx 0.03 r_{\text{AU}}^{1/4}. \quad (8)$$

The density at the midplane,  $\rho_0$ , is determined by eq (1) and the relation  $\Sigma = \sqrt{2\pi}\rho_0 h$ , yielding a number density of hydrogen nuclei

$$n_{\text{H}} = 5.8 \times 10^{14} r_{\text{AU}}^{-11/4} \text{ cm}^{-3} \quad (9)$$

at the midplane. It should be emphasised that the temperature certainly depends on height because of the effects of external irradiation, height-dependent dissipation of accretion energy and the effects of chemistry and optical depth on the ability of a gas parcel to cool (see e.g. Dullemond et al. 2007). Nevertheless the decline in pressure with height required by tidal confinement of the disk is provided primarily by the drop in density.

### 3 Magnetic field strength

There are as yet, no direct measurements of the field strength in protoplanetary disks, apart from remanent magnetism in meteorites which indicate field strengths in the solar nebula of 0.1–1 G at 1 AU (Levy & Sonett 1978). Nevertheless the likely range of field strengths is easily estimated. A lower limit is established by the 1–10 mG magnetic field strengths measured using Zeeman splitting of OH 18 cm lines in the cores of molecular clouds and in masers in star forming regions. This field is likely to be amplified by compression and shear during the formation of the central star and its surrounding disk. It therefore seems likely that

$$B \gtrsim 10 \text{ mG} \quad (10)$$

in protoplanetary disks. An upper limit on  $B$  is provided by equality of magnetic and thermal pressure in the disk midplane,

$$\frac{B_{\text{eq}}^2}{8\pi} = \rho_0 c_s^2 \quad (11)$$

which yields

$$B \lesssim B_{\text{eq}} \approx 18 r_{\text{AU}}^{-13/8} \text{ G}. \quad (12)$$

Note that the equipartition field  $B_{\text{eq}}$  scales as  $\Sigma^{1/2}$  if the disk surface density is increased over the minimum solar nebula value given by eq. (1). The upper and lower limits are disparate at 1 AU but are equal at 100 AU.

It is worth comparing these limits to the field strength that is *required* if magnetic fields are responsible for the loss of angular momentum implied

by the observationally inferred disk accretion rates  $\dot{M} \sim 10^{-7} M_{\odot} \text{ yr}^{-1}$  (Calvet, Hartmann & Strom 2000). To do this, we take as a starting point the MHD momentum equation

$$\rho \frac{\partial \mathbf{v}}{\partial t} + \rho(\mathbf{v} \cdot \nabla)\mathbf{v} + \nabla P + \rho \nabla \Phi = -\frac{\nabla B^2}{8\pi} - \frac{(\mathbf{B} \cdot \nabla)\mathbf{B}}{4\pi}, \quad (13)$$

where  $P$  is the gas pressure and  $\Phi$  is the point-mass gravitational potential of the central star. Assuming axisymmetry, and adopting cylindrical coordinates, the toroidal component of the momentum equation reduces to  $\rho[(\mathbf{v} \cdot \nabla)\mathbf{v}]_{\phi} = (\mathbf{B} \cdot \nabla)\mathbf{B}_{\phi}/4\pi$ . It is clear that the options for angular momentum transport under these assumptions are limited! Assuming that  $v_z$  is small within the disk we obtain

$$\frac{\rho v_r}{r} \frac{\partial(rv_{\phi})}{\partial r} = \frac{B_r}{4\pi r} \frac{\partial(rB_{\phi})}{\partial r} + \frac{B_z}{4\pi} \frac{\partial B_{\phi}}{\partial z}, \quad (14)$$

which equates the rate of angular momentum loss by the gas to the magnetic torque. The magnetic field transports angular momentum radially and vertically via the  $\partial/\partial r$  and  $\partial/\partial z$  terms on the right hand side respectively. The LHS is related to the accretion rate at  $r$ ,

$$\dot{M} = -2\pi r \int_{-s}^{+s} \rho v_r dz, \quad (15)$$

by integrating between the lower and upper disk surfaces at  $z = \pm s$ . Before integrating eq (14) in this manner, note that  $v_{\phi} \approx v_K \hat{\phi}$  where  $v_K = \sqrt{GM/r}$  and use  $\nabla \cdot \mathbf{B} = 0$  to obtain

$$\frac{\rho v_r v_K}{2r} \approx \frac{1}{4\pi r^2} \frac{\partial}{\partial r}(r^2 B_r B_{\phi}) + \frac{1}{4\pi} \frac{\partial}{\partial z}(B_z B_{\phi}). \quad (16)$$

Then integrating vertically between the disc surfaces yields

$$\frac{\dot{M} v_K}{2r^2} \approx \frac{1}{r^2} \frac{\partial}{\partial r}(r^2 h \langle -B_r B_{\phi} \rangle) - (B_z B_{\phi})_s \quad (17)$$

where I have defined

$$\langle -B_r B_{\phi} \rangle \equiv -\frac{1}{2h} \int_{-s}^{+s} B_r B_{\phi} dz. \quad (18)$$

and  $B_z B_{\phi} = +(B_z B_{\phi})_s$  or  $-(B_z B_{\phi})_s$  at the upper or lower disc surfaces respectively. If  $B_r$  and  $B_z$  are the same order of magnitude, and the magnetic flux exiting the disk surfaces is anchored in an external envelope or outflow, then  $B_{\phi}$  at the disk surface is non-negligible and the first term in (18) is smaller than the second by a factor  $\sim h/r$ . In this case the torque per unit area applied to the disk by the net magnetic tension

across it equals the rate of angular momentum loss by the material in the disk, and

$$\sqrt{|B_z B_\phi|_s} \approx \left( \frac{\dot{M} v_K}{2r^2} \right)^{1/2} \approx 0.2 \dot{M}_{-7}^{1/2} r_{\text{AU}}^{-5/4} \text{ G}, \quad (19)$$

where  $\dot{M}_{-7}$  is  $\dot{M}$  in units of  $10^{-7} M_\odot \text{ yr}^{-1}$ .

This estimate is a robust lower limit on the rms field in the disk, as it assumes efficient vertical transport of angular momentum by an ordered magnetic field. If radial transport dominates instead, then  $\langle -B_r B_\phi \rangle^{1/2}$  must be larger than the estimate (19) by a factor  $\sim \sqrt{r/h}$ . If the field is disordered because of turbulence, then these represent a space *and* time-averaged rms magnetic field (see, e.g. Balbus 2003), and the local field may be somewhat larger. For example, simulations of the magnetorotational instability indicate that  $B_{\text{rms}} \sim 2 \langle -B_r B_\phi \rangle^{1/2}$  (Sano et al. 2004). In any case, one concludes that Gauss-strength fields at 1 AU are required to give the inferred accretion rates.

#### 4 Magnetic diffusion

Magnetic diffusion is an essential ingredient in any theory of magnetised astrophysical disks. For example, field diffusion allows matter to be accreted while leaving the magnetic field behind. In disk-driven wind models magnetic diffusion allows some of the disk material to be loaded onto field lines and flung outwards from the disk surfaces (Wardle & Königl 1993) while the remainder is accreted. Diffusion is also associated with energy dissipation and sets the inner scale of magnetic structures.

The magnitude of the diffusivity is determined by microphysical processes rather than the wishes of a theorist (or an observer for that matter!). In fully-ionised disks the molecular diffusivity is orders of magnitude too small and an effective turbulent viscosity or anomalous diffusivity of plasma physics origin has to be invoked as the origin of the breakdown of ideal MHD. In the weakly-ionised environment of protoplanetary disks collisions between charged particles and the dominant neutrals are sufficient to provide the necessary diffusivity, and may be too efficient, suppressing magnetic activity, leading to the formation of “dead” zones in the disk (Gammie 1996; Wardle 1997). If simple neutral-charged particle collisions are the origin of diffusivity then *quantitative* calculations can provide a sound physical basis for calculations of magnetic field evolution in protoplanetary disks.

The finite conductivity of a weakly-ionised gas can be determined by calculating the drift of charged particles

in response to an applied electric field  $\mathbf{E}'$  in the neutral frame, and summing over the charged species to obtain the current (Cowling 1976). The drift velocity  $\mathbf{v}_j$  of each charged species  $j$  (mass  $m_j$ , charge  $Z_j e$ ) relative to the neutrals (mean mass  $m$ , density  $\rho$ ) is determined by balancing the force applied by the electric field, the magnetic force, and the drag associated with neutral collisions:

$$Z_j e \mathbf{E}' + Z_j e \frac{\mathbf{v}_j}{c} \times \mathbf{B} - m_j \gamma_j \rho \mathbf{v}_j = 0 \quad (20)$$

where  $\gamma_j = \langle \sigma v \rangle_j / (m_j + m)$  and  $\langle \sigma v \rangle_j$  is the rate coefficient for collisional momentum transfer between species  $j$  and the neutrals, so  $\gamma_j \rho$  is the collision frequency with neutrals. Eq (20) implicitly assumes that the electromagnetic field and the neutral fluid evolve on a time scale that is long compared to the inertial time scales of charged particles, which is generally a good approximation (see Wardle & Ng 1999). The direction of the drift of a particle of mass  $m_j$ , charge  $Z_j e$  is determined by the relative magnitude of the magnetic and drag terms in eq (20), which is characterised by the Hall parameter for species  $j$

$$\beta_j = \frac{|Z_j| e B}{m_j c} \frac{1}{\gamma_j \rho} \quad (21)$$

i.e. the ratio of the gyrofrequency and neutral collision frequency<sup>1</sup>. Note that apart from molecular factors, the Hall parameter depends only on  $B/n_{\text{H}}$ . If  $\beta_j \gg 1$  the Lorentz force dominates the neutral drag

$$Z_j e \mathbf{E}' \approx -Z_j e \frac{\mathbf{v}_j}{c} \times \mathbf{B} \quad (22)$$

and the charged particles are tied to the magnetic field lines. In the other limit  $\beta_j \ll 1$  the drag dominates

$$Z_j e \mathbf{E}' \approx \gamma_j m_j \rho \mathbf{v}_j \quad (23)$$

and neutral collisions completely decouple the particles from the magnetic field.

Inverting eq (20) for  $\mathbf{v}_j$ , and forming the current density  $\mathbf{J} = \sum_j n_j e Z_j \mathbf{v}_j$  yields

$$\mathbf{J} = \sigma_O \mathbf{E}'_{\parallel} + \sigma_H \hat{\mathbf{B}} \times \mathbf{E}'_{\perp} + \sigma_P \mathbf{E}'_{\perp} \quad (24)$$

where  $\mathbf{E}'_{\parallel}$  and  $\mathbf{E}'_{\perp}$  are the components of  $\mathbf{E}'$  parallel and perpendicular to  $\mathbf{B}$  and the ohmic, Hall, and Pedersen conductivities are (e.g. Cowling 1976; Wardle & Ng 1999):

$$\sigma_O = \frac{ec}{B} \sum_j n_j |Z_j| \beta_j, \quad (25)$$

<sup>1</sup>Note that Wardle & Ng (1999) include the sign of  $Z_j$  in the definition of  $\beta_j$

$$\sigma_H = -\frac{ec}{B} \sum_j \frac{n_j Z_j \beta_j^2}{1 + \beta_j^2} = \frac{ec}{B} \sum_j \frac{n_j Z_j}{1 + \beta_j^2} \quad (26)$$

and

$$\sigma_P = \frac{ec}{B} \sum_j \frac{n_j |Z_j| \beta_j}{1 + \beta_j^2} \quad (27)$$

respectively, where I have used  $\sum n_j Z_j = 0$  in deriving the second form of  $\sigma_H$  in eq (26).

Inverting eq (26) for  $\mathbf{E}'$  yields an induction equation of the form

$$\frac{\partial \mathbf{B}}{\partial t} = \nabla \times (\mathbf{v} \times \mathbf{B}) - \nabla \times [\eta_O \nabla \times \mathbf{B} + \eta_H (\nabla \times \mathbf{B}) \times \hat{\mathbf{B}} + \eta_A (\nabla \times \mathbf{B})_{\perp}] \quad (28)$$

where

$$\eta_O = \frac{c^2}{4\pi\sigma_O}, \quad (29)$$

$$\eta_H = \frac{c^2}{4\pi\sigma_{\perp}} \frac{\sigma_H}{\sigma_{\perp}}, \quad (30)$$

and

$$\eta_A = \frac{c^2}{4\pi\sigma_{\perp}} \frac{\sigma_P}{\sigma_{\perp}} - \eta_O \quad (31)$$

are the ohmic, Hall and ambipolar diffusivities respectively, where  $\sigma_{\perp} = \sqrt{\sigma_H^2 + \sigma_P^2}$ .

If the only charged particles are ions and electrons, then  $\eta_H = \beta_e \eta_O$  and  $\eta_A = \beta_i \beta_e \eta_O$ . The Hall parameters for ions and electrons are

$$\beta_i \approx 4.6 \times 10^{-3} \frac{B_G}{n_{15}} \quad (32)$$

and

$$\beta_e \approx 3.5 \frac{B_G}{n_{15}} \left( \frac{T}{100 \text{ K}} \right)^{-1/2} \quad (33)$$

respectively, where  $B_G$  is the magnetic field in Gauss and  $n_{15} = n_H/10^{15} \text{ cm}^{-3}$ . As  $\beta_e/\beta_i \sim 1000$  there are three distinct diffusion regimes:

$$\begin{aligned} \beta_i \ll \beta_e \ll 1 & \quad \text{ohmic (resistive)} \\ \beta_i \ll 1 \ll \beta_e & \quad \text{Hall} \\ 1 \ll \beta_i \ll \beta_e & \quad \text{ambipolar} \end{aligned} \quad (34)$$

which correspond to different regimes of  $B/n_H$ , as illustrated in Figure 1. In the ohmic regime, the ion and electron drifts are unaffected by the magnetic field,

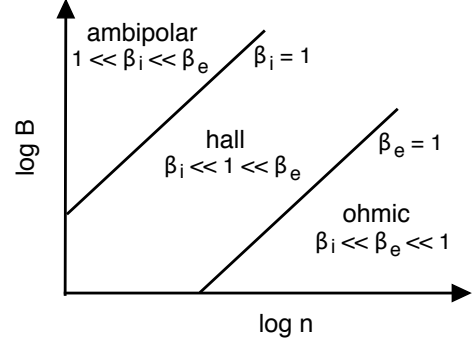


Fig. 1.— The magnetic diffusion regimes of a weakly-ionised, three-component plasma are determined by the ion and electron Hall parameters  $\beta_i$  and  $\beta_e$ , which are proportional to  $B/n$ , with  $\beta_e/\beta_i$  typically  $\sim 1000$  (see text).

in the Hall regime the electrons are tied to the field but the ions are not, while in the ambipolar diffusion regime both species are tied to the magnetic field and drift together through the neutrals. The presence of grains complicates this picture (Wardle & Ng 1999), but generically ohmic or ambipolar diffusion dominates if the majority of charged particles are tied to the neutrals or the magnetic field respectively, otherwise Hall diffusion is important.

Which diffusion regimes are relevant? Figure 2 plots the loci in the  $\log B$ – $\log n_H$  plane where the Hall parameters are unity for ions, electrons, and singly-charged grains with radii of 50 and 2500 Å. Also shown are the regions occupied by molecular clouds ( $B[\text{mG}] \sim \sqrt{n_H[\text{cm}^{-3}]}$ ) and the midplane of the solar nebula (eqs [9] and [12]) between 1 and 100 AU. Densities are so large at the midplane of the solar nebula that ions are decoupled from the magnetic field by neutral collisions. This is not so for electrons except for very weak fields, and so Hall diffusion is important once grains have settled or aggregated and are not the dominant charge carriers. If grains are important they are very much decoupled from the magnetic field (i.e.  $\beta_g \ll 1$ ) and ohmic diffusion dominates. However, the diffusivity is then so severe that the magnetic field cannot couple effectively to the gas at all (Hayashi 1981).

By contrast, in molecular clouds ions and electrons are tied to magnetic fields whereas the largest grains are not. The charge residing on large grains is usually small except inside shock waves (Wardle & Chapman 2006) or at very high densities. Thus in molecular clouds, ambipolar diffusion dominates.

How much diffusion in protoplanetary disks is too much of a good thing? This depends on the scale on which one would like the magnetic field to couple to

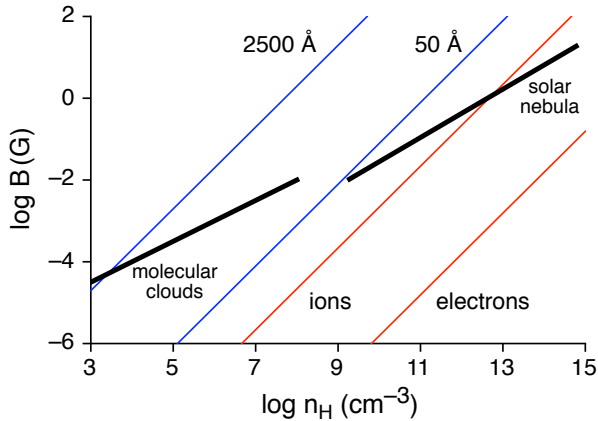


Fig. 2.— Loci in the  $\log B$ - $\log n_{\text{H}}$  plane where the Hall parameters are unity for ions and electrons (red) and 50 and 2500 Å grains (blue). Thick black lines indicate the region occupied by molecular clouds ( $B[\text{mG}] \sim \sqrt{n_{\text{H}}[\text{cm}^{-3}]}$ ) and the equipartition field at the mid-plane of the minimum-mass solar nebula between 1 and 100 AU.

the matter in the disk. The weakest criterion for interesting magnetic effects is to demand that the magnetic field should at least be able to couple to the Keplerian shear in the disk. This is required both by the magnetorotational instability and by disk-driven wind models. To estimate this, consider the induction equation (28). The magnitude of the inductive term  $|\nabla \times (\mathbf{v} \times \mathbf{B})| \sim \Omega B$ , where  $\Omega = v_K/r = c_s/h$  is the Keplerian frequency. The diffusive term is dominated by vertical gradients, and so  $|\nabla \times (\eta \nabla \times \mathbf{B})| \sim \eta B/h^2$  where  $\eta$  is the largest of  $\eta_O$ ,  $|\eta_H|$  and  $\eta_A$ . The diffusion term must be smaller than the advective term to allow the field to couple to the Keplerian shear, corresponding to the requirement

$$\eta \lesssim hc_s \quad (35)$$

for good coupling.

## 5 Diffusivity calculations

To answer the question of whether the magnetic diffusivity is too low or high, and which diffusion mechanism dominates in different regions of protoplanetary disks, we must calculate the ohmic, Hall and ambipolar diffusivities appearing in eq (28). These depend on the abundances of the charged species and their Hall parameters (see eqs [29]–[31]).

To calculate the charged particle abundances at a given radius we adopt the surface density and temperature of the minimum solar nebula, and assume that it

is isothermal in the  $z$ -direction. The ionising sources are radioactivity (which is largely negligible), cosmic rays, and the x-ray flux from the central star. The cosmic ray flux is assumed to induce an ionisation rate  $10^{-17} \text{ s}^{-1} \text{ H}^{-1}$  well outside the disk and suffers exponential attenuation with depth as  $\exp(-\Sigma/96 \text{ g cm}^{-2})$  (Umebayashi & Nakano 1981). For the depth dependence of the x-ray ionisation we adopt a fit to the results of Igea & Glassgold (1999). The simple chemical reaction scheme of Nishi, Nakano & Umebayashi (1991) and Sano et al. (2000) is adopted, which follows the abundances of the light ions  $\text{H}^+$ ,  $\text{H}_3^+$ ,  $\text{He}^+$ ,  $\text{C}^+$ , and representative heavier molecular and metal ions (denoted  $m^+$  and  $M^+$  respectively), as well as charged grains. Their scheme has been extended to include high grain charge using the cross sections of Draine & Sutin (1987). This is necessary because the temperatures here are high compared to molecular clouds – the high thermal velocities of electrons can overcome large Coulomb barriers allowing grains to pick up a high charge through electron sticking. Following Umebayashi & Nakano (1990) I consider populations of uniform size grains, as well as models in which grains have settled out.

A sophisticated treatment of the ionisation equilibrium using a full chemical reaction network has been performed by Semenov, Wiebe & Henning (2004), although with a more restricted treatment of grain charging.

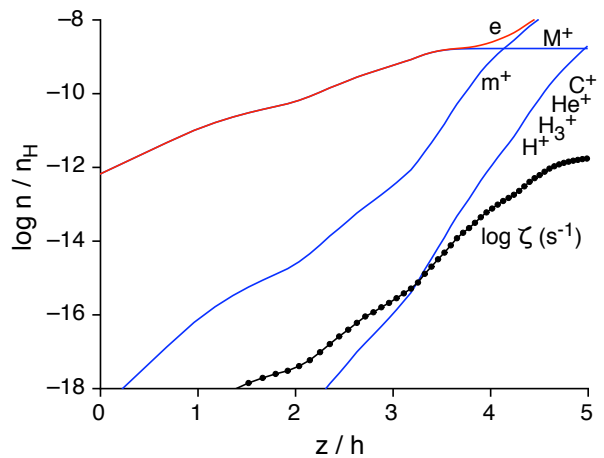


Fig. 3.— Ionisation rate (black dotted curve) and fractional abundance (relative to hydrogen nuclei) of ions (blue) and electrons (red) as a function of height above the midplane,  $z$ , in the minimum solar nebula at 1 AU from the central star. Grains are assumed to have aggregated and settled to the midplane.

Figure 3 shows the ionisation rate and abundances at 1 AU as a function of height  $z$  from the midplane in

the absence of grains (i.e. once they have settled). The ionisation rate is dominated by x-rays above  $z/h = 2$ , and by cosmic rays at greater depths. The dominant charged species are electrons and metal ions because the recombination rate coefficient for metal ions is two orders of magnitude below that for molecular ions. The ionisation fraction declines with depth because of the decreasing ionisation rate and increasing neutral density.

Figure 4 shows the corresponding ohmic, Hall and ambipolar diffusivities as a function of height for field strengths of 0.1 and 1 G. The ohmic resistivity is independent of the magnetic field strength, whereas the Hall and ambipolar diffusivities scale linearly and quadratically with  $B$  respectively. The ohmic diffusivity is proportional to  $n_e$  and declines strongly with height. The ion and electron Hall parameters, which are inversely proportional to  $\rho$ , increase strongly with height. As a result, the Hall and ambipolar diffusivities increase above  $z/h \sim 2$  where the neutral density starts to drop rapidly. Hall diffusion dominates below 2-3 scale heights, and ambipolar diffusion dominates at greater heights. Note that the magnetic field is able to couple to the shear in the disk below 3-4 scale heights. Above this, ambipolar diffusion is severe. At first sight this is counter-intuitive – the diffusion is most severe above the disk where the ionising flux is strongest and the fractional ionisation is greatest! The problem is that the *number density* of charged particles is very low at the disk surface.

Figure 5 extends this plot to other values of  $B$  by representing the diffusivity as contours of  $(\eta_O^2 + \eta_H^2 + \eta_A^2)^{1/2}$  in a  $\log B$ - $z/h$  plane, with the background colour indicating the dominant diffusion mechanism. The curves in Figure 4 correspond to horizontal cuts in this plane at  $\log B(G) = 0$  and  $-1$ . It is clear that ohmic diffusion is important only for weak fields near the midplane (i.e. when  $\beta_e \lesssim 1$ ), whereas ambipolar diffusion is dominant at the disk surface and for stronger fields (when  $\beta_i \gg 1$ ). Hall diffusion dominates over the large range of intermediate conditions.

If we add a standard interstellar population of  $0.1 \mu\text{m}$  radius grains, the ionisation equilibrium is very different (Fig. 6) because the grains acquire a charge via sticking of electrons and ions from the gas phase. Above  $z/h \approx 4$  the grain charge is determined by the competitive rates of sticking of ions and electrons. The mean grain charge,  $\approx -7e$ , is determined by the Coulomb repulsion of electrons offsetting their greater thermal velocity compared to ions. Most recombinations still occur in the gas phase. For  $z/h \approx 3$ -3.5, the abundances of ions and electrons have declined to the point that the majority of electrons stick to grain surfaces be-

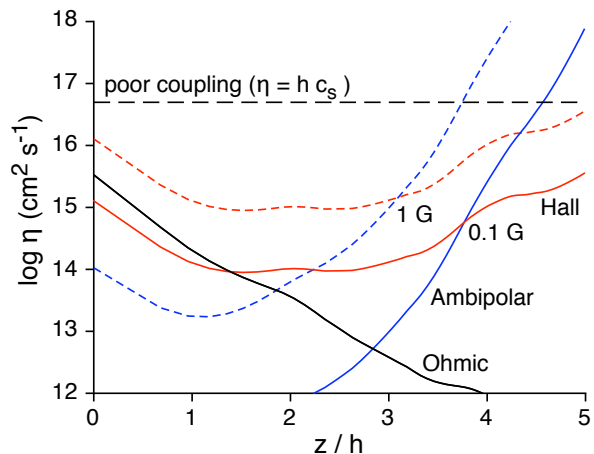


Fig. 4.— Magnetic diffusivities (ohmic – *black* curve; Hall – *red* curves; ambipolar – *blue* curves) as a function of height above the midplane derived from the charged particle abundances plotted in Fig. 3 for magnetic field strengths of 0.1 and 1 G (*solid* and *dashed* curves respectively). A single curve for ohmic diffusivity is plotted as this does not depend on  $B$ . The horizontal dashed line indicates the value of diffusivity at which the magnetic field is unable to effectively couple to the Keplerian shear in the disk (see §4).

fore they can recombine in the gas phase, and most neutralisations occur when ions stick to negatively charged grains. Closer to the midplane, the ionisation fraction is so low that most grains are neutral, and ions typically stick to a neutral grain before encountering a negatively charged grain. Recombinations mostly occur in this region through the collision of positive and negative grains. These regimes were found by Umebayashi & Nakano (1990), and as expected the curves are similar to theirs (except for the large grain charge for  $z/h \gtrsim 3$ ) when the abundances are plotted as a function of  $\zeta/n_H$  rather than  $z/h$ .

Grains severely decrease the conductivity by reducing the abundance of charged particles and because of their much reduced mobility relative to ions and especially electrons. Figure 7 shows the diffusivity as a function of height for field strengths of 0.1 and 1 G. Close to the midplane the diffusivity is increased by 7-8 orders of magnitude compared to the case when grains are absent. It is only for the weaker field and  $z/h \gtrsim 3.5$  that the diffusivity is low enough to allow the magnetic field to couple to the disk. The diffusivity as a function of  $z/h$  and field strength is plotted in Figure 8. The vertical contours on the left hand half of the plane (i.e. for  $z/h \lesssim 3$  reflect the strong decline of the conductivity towards the midplane as the density

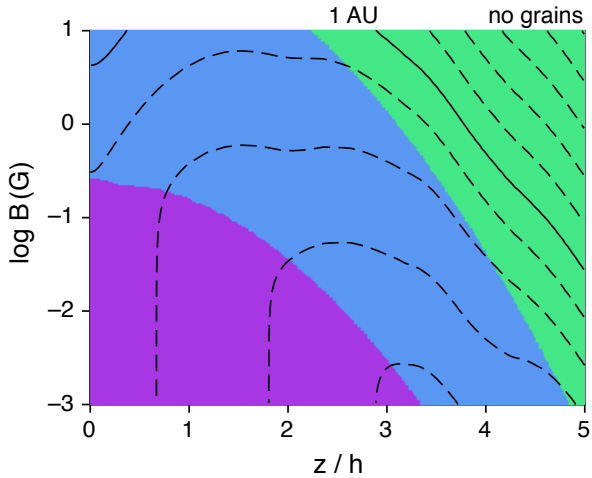


Fig. 5.— Logarithmically-spaced contours of  $(\eta_{\text{O}}^2 + \eta_{\text{H}}^2 + \eta_{\text{A}}^2)^{1/2}$  as a function of height and magnetic field strength at 1 AU in the minimum mass solar nebula. The charged particle abundances are plotted in Figure 3. The contour levels increase by factors of 10 from  $10^{-4} hc_s$  at the bottom of the plot near  $z/h = 3$  up to  $10^5 hc_s$  at the very top right-hand corner of the plot. The solid contour is the critical value  $hc_s$  – in the region above this contour the magnetic field cannot couple effectively to the disk. The background shading indicates whether the dominant diffusion mechanism is ohmic (*purple*), Hall (*blue*) or ambipolar (*green*).

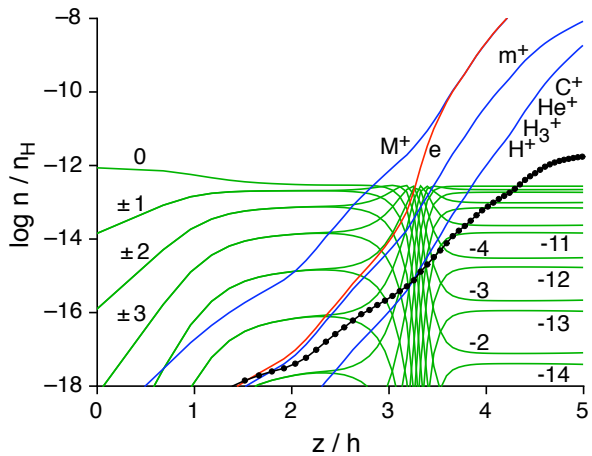


Fig. 6.— As for Fig. 3, but including a standard interstellar population of  $0.1 \mu\text{m}$  radius grains. *Green* curves indicate the abundances of different grain charge states  $Ze$ , labelled by  $Z$ .

(and therefore neutral drag) increases and the number of charge carriers decreases. For weak to moderate fields the dominant charge carriers – i.e the grains – are

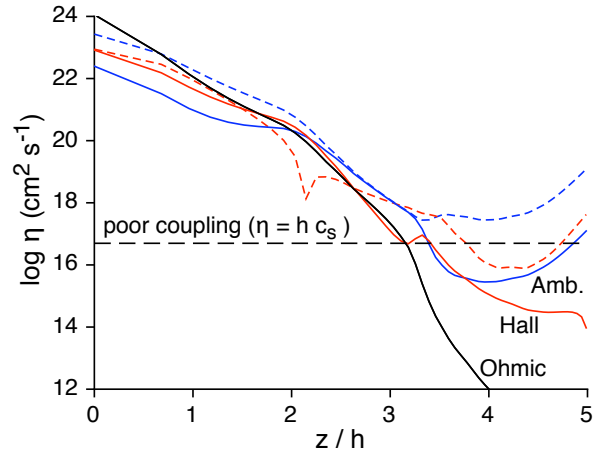


Fig. 7.— As for Fig. 4 but for the charged particle abundances plotted in Fig. 6. Note that the vertical scale extends to much larger values than that in Fig. 4 because the dominance of charged grains for  $z/h \lesssim 3.5$  increases the diffusivity by many orders of magnitude. The kink in the dashed red curve at  $z/h \approx 2.2$  occurs because for  $B = 1 \text{ G}$  the Hall diffusivity becomes negative above this point (the absolute value is plotted).

decoupled from the magnetic field by neutral collisions and ohmic diffusion dominates. The grains become tied to the magnetic field if it is strong enough and ambipolar diffusion dominates. Hall diffusion, which would normally be prominent at intermediate field strengths, is suppressed by the almost equal numbers of positive and negative grains. This is because the Hall effect relies on different degrees of field line-tying for positive and negatively charged species. Above  $z/h \approx 3.5$  where grains become unimportant, the diffusivity behaves as in Figure 5. The region where the magnetic field can couple to the differential rotation of the disk is restricted to  $B \lesssim 0.5 \text{ G}$  and  $z/h \approx 3.5\text{--}5$ .

These effects can be mitigated by the aggregation of grains, which reduce the surface area available to capture charged particles from the gas phase. For example, I show in Figure 9 the diffusivities obtained if grains have aggregated to  $3 \mu\text{m}$  in radius. This is sufficient to allow the coupled region to extend down to  $z/h \approx 1.5$ , which is now the height below which the grains dominate the charged species. Grains rapidly grow to this size in protoplanetary disks, so this suggests that Gauss-strength magnetic fields can couple to 10% of the disk at 1 AU.

At 5 AU, the region of giant planet formation, the x-ray flux is reduced by a factor of about 25, while the column density,  $\approx 60 \text{ g cm}^{-2}$ , is no longer able to significantly attenuate the cosmic ray flux impinging on the midplane. The ionisation rate drops from

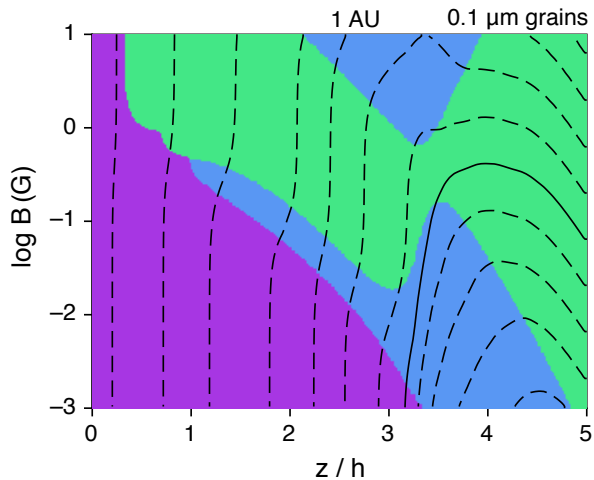


Fig. 8.— As for Fig. 5, but for the charged particle abundances plotted in Fig. 6 (i.e. including  $0.1 \mu\text{m}$  radius grains.)

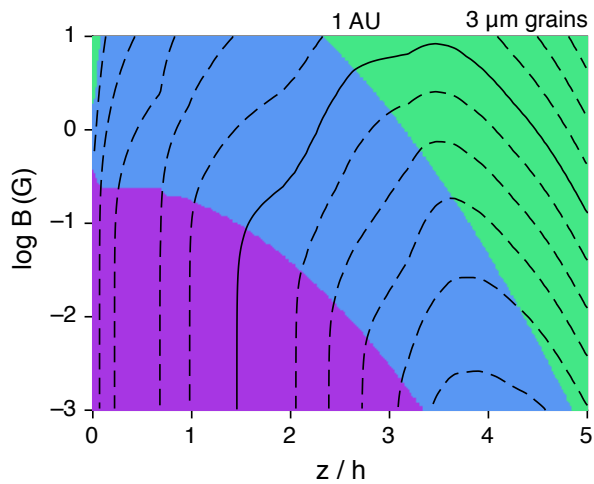


Fig. 9.— As for Fig. 5, but assuming that grains have radius  $3 \mu\text{m}$ .

$\sim 10^{-13} \text{ s}^{-1} \text{ H}^{-1}$  at the surface to  $\sim 10^{-17} \text{ s}^{-1} \text{ H}^{-1}$  at the midplane. The ionisation fraction is similar to that at 1 AU, but the reduced gas density allows greater mobility of ions and electrons. Equipartition fields ( $\sim 1 \text{ G}$ ) can easily couple to the midplane in the absence of grains (see Fig. 10). Note that Hall diffusion tends to dominate.

Grains, if present, increase the diffusion and create a dead zone, though not as extensive as that at 1 AU. Increasing the grain size to just  $1 \mu\text{m}$  is sufficient to move the transition from gas-phase to grain-dominated recombinations down to the midplane. Then magnetic fields with strengths below a few tens of milliGauss can

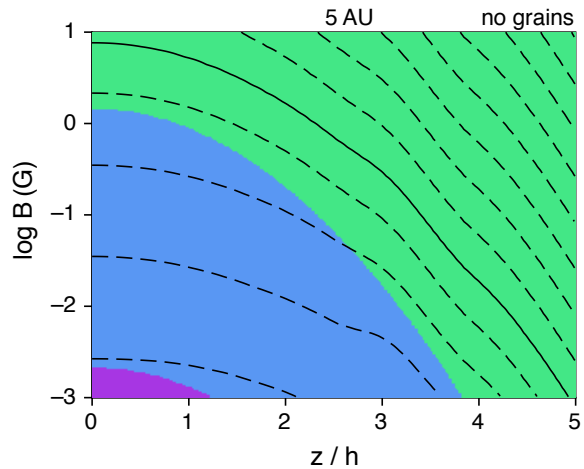


Fig. 10.— As for Fig. 5, but at 5 AU in the minimum solar nebula in the absence of grains.

couple to the bulk of the disk (Fig. 11) and Hall diffusion again is dominant.

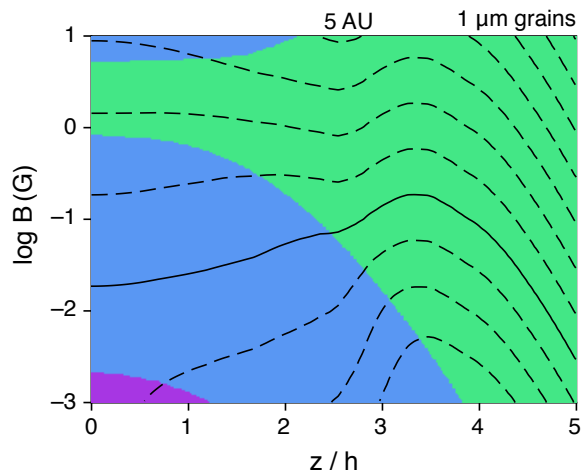


Fig. 11.— As for Fig. 5, but at 5 AU in the minimum solar nebula and assuming that grains have radius  $1 \mu\text{m}$ .

## 6 Discussion

These resistivity calculations assume a minimum-mass solar nebula subject to cosmic-ray and x-ray ionisation, with grains (if present) assumed to be of uniform size. Here I discuss the effect of relaxing these assumptions.

First, it is not at all clear that protoplanetary disks are subject to ionisation by interstellar cosmic rays because super-Alfvénic winds may advect them away from the disk (as noted by Gammie 1996 and Glassgold et al. 1997), or they may be excluded by unfavourable

magnetic geometry such as hour-glass shaped magnetic field lines vertically threading the disk or a wound-up field lying in the disk plane. This may be compensated by cosmic rays produced by magnetic activity near the central star or in a disk corona, but it is also unclear whether these particles are able to impinge on the disk. If cosmic rays are absent then the only significant ionisation source are x-rays from the central star. Naively one might think that the active layer is then restricted to the nominal penetration depth of x-rays, i.e.  $\sim 1.4 m_{\text{H}}/\sigma_T \sim 3.5 \text{ g cm}^{-2}$ . However, the x-ray induced active layer is much deeper than this because the unattenuated x-ray ionisation rate is so high – x-ray ionisation dominates for  $z/h \gtrsim 2$ . I find that in the absence of dust grains, the active column density is  $\Sigma_{\text{active}} \approx 150 \text{ g cm}^{-2}$ . When dust grains are present the active layer lies within the region where x rays dominate cosmic rays in any case, so this case is unaffected by eliminating the cosmic rays.

Second, the calculations presented here adopt the surface density for the minimum-mass solar nebula. While this is broadly consistent with observed protoplanetary disks (Kitamura et al. 2002), it is possible to have surface densities 30-50 times higher without suffering gravitational instability. The approximate effect of adding material to the disk is to multiply up the density everywhere by the same factor. The dominant factor in the ionisation equilibrium is the shielding of the ionising fluxes of cosmic and x-rays by the overlying column of disk material. To a first approximation the active column densities discussed above are unchanged.

Third, I have implicitly used single size grain models to crudely mimic the effect of aggregation. Some care is needed in interpreting these results because of the tendency for the smallest grains to carry a significant fraction of the grain charge. For example, although the typical grain size increases to micron scales on times that are short compared to the disk evolutionary time scale, the residual small grains implied by any stochastic aggregation process may still be important (see, e.g. Nomura & Nakagawa 2006). The primary role of grains is to mop up electrons from the gas phase and render them immobile, increasing the magnetic diffusivity by many orders of magnitude. This effect is significant below the transition layer where the charge density of electrons and grains are comparable (e.g. at  $z/h \approx 3.5$  in Fig. 6). Above this transition, the charge residing on grains is unimportant in determining the abundances of ions and electrons and their occasional sticking onto grains yields a mean charge  $Z_g(a) e \approx -4kTa/e$  on grains of radius  $a$  (Spitzer 1941; Draine & Sutin 1987). The total charge per unit volume carried by grains with a size distribution  $x_g(a)$  (where the number density of grains with

radii between  $a$  and  $a + da$  is  $n_{\text{H}}x_g(a) da$ ) is therefore  $\int x_g(a)Z_g(a) da$ . The transition from low to high diffusivity occurs when the charge per hydrogen nucleus on grains becomes comparable to that in electrons, so the height of the magnetically active surface layer ( $z_{\text{mag}}$ , say) is a weak, monotonically increasing function of  $\int a x_g(a) da$ . The results presented for the  $3 \mu\text{m}$  and  $0.1 \mu\text{m}$  grain models show that  $z_{\text{mag}}/h \sim 2.2$  and  $3.5$  for  $\int a x_g(a) da = 8.9 \times 10^{-18} \text{ cm}$  and  $9.9 \times 10^{-21} \text{ cm}$  respectively. By way of comparison, 1% of the total grain mass residing in  $0.01 \mu\text{m}$  grains would carry approximately the same net charge as the  $0.1 \mu\text{m}$  grain population so a trace residual population of small grains may poison the magnetically coupled layer.

Finally, although the fractional ionisation increases with height above the disk the diffusivity also increases. This is because the number density of charged particles plummets because the density is dropping as  $\exp(-z^2/2h^2)$ . This potentially affects the ability to drive a wind from the disk surface. However it should be noted that the density profile at large heights becomes increasingly unreliable due to the effects of temperature stratification and/or the presence of outflows.

## 7 Summary

If dust grains have settled to the midplane, or have otherwise been removed from the gas, the ionisation level in the disk is sufficient to couple the magnetic field can to the midplane even within 1 AU of the central star. In this case the column density of the magnetically active region of the disk is  $\Sigma_{\text{active}} \approx 1700 \text{ g cm}^{-2}$ . Hall diffusion dominates (Wardle & Ng 1999; Sano & Stone 2002) because the ions are decoupled from the magnetic field and electrons are not. Notably, the Hall effect imparts an implicit handedness to the fluid dynamics, which becomes sensitive to a global reversal of the magnetic field direction.

Dust grains, if present, substantially increase magnetic diffusion by soaking up electrons and ions from the gas phase. Grains have huge cross sections for neutral collisions and this combined with their large inertia effectively decouples them from the magnetic field and the fluid becomes resistive. Magnetic diffusion is so severe that the field is unable to couple to the shear in the disk except close to the disk surface. For a standard interstellar population of  $0.1 \mu\text{m}$ -radius grains the active surface layers have a combined total column  $\Sigma_{\text{active}} \approx 2 \text{ g cm}^{-2}$ . As grains aggregate, their effect on the ionisation equilibrium is reduced, and by the time grains have aggregated to  $3 \mu\text{m}$ ,  $\Sigma_{\text{active}} \approx 80 \text{ g cm}^{-2}$ . At 5 AU the lower column density and reduced gas density

and shear means that the coupling is more easily maintained. In this case  $\Sigma_{\text{active}} \approx \Sigma_{\text{total}}$  once grains have aggregated to  $1 \mu\text{m}$  in size.

If a substantial grain population is present, ionisation in the magnetically active layers is dominated by x-rays so that there is little change if cosmic rays are unable to impinge on the disk. In the absence of grains and cosmic rays, stellar x-rays maintain magnetic coupling to 10% of the disk material at 1 AU (i.e.  $\Sigma_{\text{active}} \approx 150 \text{ g cm}^{-2}$ ) and almost all of it at 5 AU once grains have aggregated or been removed by settling, which is expected to happen on a time scale of a few thousand years (e.g. Nomura & Nakagawa 2006).

## References

- Andrews, S. M., Williams, J. P.: Circumstellar dust disks in Taurus-Auriga: the submillimeter perspective. *Astrophys. J.* **631**, 1134–1160 (2005)
- Balbus, S. A.: Enhanced angular momentum transport in accretion disks. *Ann. Rev. Astron. Astrophys.* **41**, 555–597 (2003)
- Balbus, S. A., Hawley, J. F.: A powerful local shear instability in weakly magnetized disks: I. Linear analysis. *Astrophys. J.* **376**, 214–233 (1991)
- Balbus, S. A., Terquem, C.: Linear analysis of the Hall effect in protostellar disks. *Astrophys. J.* **552**, 235–247 (2001)
- Blandford, R. D., Payne, D. G.: Hydromagnetic flows from accretion disks and the production of radio jets. *Mon. Not. Roy. Astron. Soc.* **199**, 883–903 (1982)
- Calvet, N., Hartmann, L., Strom, S. E.: Evolution of disk accretion. In: Mannings, V., Boss, A. P., Russell, S. S. (eds.) *Protostars and Planets IV*, pp. 377–400. University of Arizona Press, Tucson (2000)
- Chambers, J. E.: Planet formation with migration. *Astrophys. J.* **652**, L133–L136 (2006)
- Chapman, J. F., Wardle, M.: Dust grain dynamics in C-type shock waves in molecular clouds. *Mon. Not. Roy. Astron. Soc.* **371**, 513–529 (2006)
- Ciesla, F. J.: Dust coagulation and settling in layered protoplanetary disks. *Astrophys. J.* **654**, L159–L162 (2007)
- Cowling, T. G., *Magnetohydrodynamics*. Hilger, London (1976)
- Draine, B. T., Sutin, B.: Collisional charging of interstellar grains. *Astrophys. J.* **320**, 803–817 (1987)
- Dullemond, C. P., Hollenbach, D., Kamp, I., D’Alessio, P.: Models of the structure and evolution of protoplanetary disks. In: Reipurth, B., Jewitt, D., Keil, K. (eds.) *Protostars and Planets V*, pp. 555–572. University of Arizona Press, Tucson (2007)
- Durisen, R. H., Boss, A. P., Mayer, L., Nelson, A. F., Quinn, T., Rice, W. K. M.: Gravitational instabilities in gaseous protoplanetary disks and implications for giant planet formation. In: Reipurth, B., Jewitt, D., Keil, K. (eds.) *Protostars and Planets V*, pp. 607–622. University of Arizona Press, Tucson (2007)
- Fendt, C.: Magnetically driven outflows from Jovian circum-planetary accretion disks. *Astron. Astrophys.* **411**, 623–635 (2003)
- Fleming, T., Stone, J. M.: Local magnetohydrodynamical models of layered accretion disks. *Astrophys. J.* **585**, 908–920 (2003)
- Fromang, S., Papaloizou, J.: Dust settling in local simulations of turbulent protoplanetary disks. *Astron. Astrophys.* **452**, 751–762 (2006)
- Gammie, C. F.: Layered accretion in T Tauri disks. *Astrophys. J.* **457**, 355–362 (1996)
- Glassgold, A. E., Najita, J., Igea, J.: X-ray ionization of protoplanetary disks. *Astrophys. J.* **480**, 344–350 (1997)
- Hawley, J. F., Gammie, C. F., Balbus, S. A.: Local three-dimensional magnetohydrodynamic simulations of accretion disks. *Astrophys. J.* **440**, 742–763 (1995)
- Hayashi, C.: Structure of the solar nebula, growth and decay of magnetic fields and effects of magnetic and turbulent viscosities on the nebula. *Prog. Theor. Phys. Supp.* **70**, 35–52 (1981)
- Igea, J., Glassgold, A. E.: X-ray ionization of the disks of young stellar objects. *Astrophys. J.* **518**, 848–858 (1999)
- Ilgner, M., Nelson, R. P.: On the ionisation fraction in protoplanetary disks. I. Comparing different reaction networks. *Astron. Astrophys.* **445**, 205–222 (2006)
- Johansen, A., Klahr, H.: Dust diffusion in protoplanetary disks by magnetorotational turbulence. *Astrophys. J.* **634**, 1353–1371 (2005)
- Johnson, E. T., Goodman, J., Menou, K.: Diffusive migration of low-mass protoplanets in turbulent disks. *Astrophys. J.* **647**, 1413–1425 (2006)
- Kitamura, Y., Momose, M., Yokogawa, S., Kawabe, R., Tamura, M., Ida, S.: Investigation of the physical properties of protoplanetary disks around T Tauri stars by a 1 arcsecond imaging survey: evolution and diversity of the disks in their accretion stage. *Astrophys. J.* **581**, 357–380 (2002)
- Levy, E. H., Sonett, C. P.: Meteorite magnetism and early solar system magnetic fields. In: Gehrels, T. (ed.) *Protostars and Planets: Studies of Star Formation and of the Origin of the Solar System*, pp. 516–532. University of Arizona Press, Tucson (1978)
- Matsumura, S., Pudritz, R. E.: The origin of Jovian planets in protostellar disks: the role of dead zones. *Astrophys. J.* **598**, 645–656 (2003)
- Nishi, R., Nakano, T., Umebayashi, T.: Magnetic flux loss from interstellar clouds with various grain-size distributions. *Astrophys. J.* **368**, 181–194 (1991)
- Nomura, H., Nakagawa, Y.: Dust size growth and settling in a protoplanetary disk. *Astrophys. J.* **640**, 1099–1109 (2006)
- Quillen, A. C., Trilling, D. E.: Do Proto-jovian Planets Drive Outflows? *Astrophys. J.* **508**, 707–713 (1998)
- Sano, T., Inutsuka, S.-I., Turner, N. J., Stone, J. M.: Angular momentum transport by magnetohydrodynamic turbulence in accretion disks: gas pressure dependence of the saturation level of the magnetorotational instability. *Astrophys. J.* **605**, 321–339 (2004)

- 
- Sano, T., Miyama, S. M., Umebayashi, T., Nakano, T.: Magnetorotational instability in protoplanetary disks. II. Ionization state and unstable regions. *Astrophys. J.* **543**, 486–501 (2000)
- Sano, T., Stone, J. M.: The effect of the Hall term on the nonlinear evolution of the magnetorotational instability. I. Local axisymmetric simulations. *Astrophys. J.* **570**, 314–328 (2002)
- Semenov, D., Wiebe, D., Henning, T.: Reduction of chemical networks. II. Analysis of the fractional ionisation in protoplanetary discs. *Astron. Astrophys.* **417**, 93–106 (2004)
- Semenov, D., Wiebe, D., Henning, T.: Gas-phase CO in protoplanetary disks: a challenge for turbulent mixing. *Astrophys. J.* **647**, L57–L60 (2006)
- Spitzer, L., Jr.: The dynamics of the interstellar medium. I. Local equilibrium. *Astrophys. J.* **93**, 369 (1941)
- Toomre, A.: On the gravitational stability of a disk of stars. *Astrophys. J.* **139**, 1217–1238 (1964)
- Turner, N. J., Willacy, K., Bryden, G., Yorke, H. W.: Turbulent mixing in the outer solar nebula. *Astrophys. J.* **639**, 1218–1226 (2006)
- Umebayashi, T., Nakano, T.: Fluxes of energetic particles and the ionization rate in very dense interstellar clouds. *Publ. Astron. Soc. Jpn.* **33**, 617 (1981)
- Umebayashi, T., Nakano, T.: Magnetic flux loss from interstellar clouds. *Mon. Not. Roy. Astron. Soc.* **243**, 103–113 (1990)
- Wardle, M.: Magnetically-driven winds from protostellar disks. In: Wickramasinghe, D., Ferrario, L., Bicknell, G. (eds.) *Accretion Phenomena and Related Outflows*. Proc. IAU Colloq. vol. 163, pp. 561–565. Astronomical Society of the Pacific, San Francisco (1997)
- Wardle, M.: The Balbus-Hawley instability in weakly ionised discs. *Mon. Not. Roy. Astron. Soc.* **307**, 849–856 (1999)
- Wardle, M., Königl, A.: The structure of protostellar accretion disks and the origin of bipolar flows. *Astrophys. J.* **410**, 218–238 (1993)
- Wardle, M., Ng, C.: The conductivity of dense molecular gas. *Mon. Not. Roy. Astron. Soc.* **303**, 239–246 (1999)
- Weidenschilling, S. J.: The distribution of mass in the planetary system and solar nebula. *Astrophys. Space Sci.* **51**, 153–158 (1977)